Modeling and Evaluation of Diode Reverse Recovery in Discrete-Transition Simulators

Natan Krihely and Sam Ben-Yaakov, *Fellow, IEEE*

Power Electronics Laboratory, Department of Electrical and Computer Engineering
Ben-Gurion University of the Negev, P.0.Box 653, Beer-Sheva 84105, ISRAEL
Tel: +972-8-6461561; Fax: +972-8-6472949;
E-mails: krikali@ee.bgu.ac.il, sby@ee.bgu.ac.il;
Website: http://www.ee.bgu.ac.il/~pel

***Abstract* -- Discrete transition simulators usually do not apply full physical models of devices and as a result, they are incapable of showing parasitic processes such as diode reverse recovery. The main objective of this study was to develop a behavioral model of diode reverse recovery that can be implemented in these simulators. The proposed model is based on the lumped charge control concept. It can be easily extracted from a simple measurement and it does not require heavy computational resources. The model was tested within the PSIM platform and was verified experimentally for various turn-off conditions. Model application is exemplified by investigating a lossless snubber of a three-phase buck-type rectifier.**

***Index Terms*— Power semiconductor diodes, modeling, Spice, snubbers, discrete event simulation.**

I. INTRODUCTION

Power electronics simulators can be divided into two groups with respect to the numerical algorithm used by them. One class are the SPICE [Berkeley SPICE2] based simulators such as Orcad [1]. SPICE uses an adjustable step, Newton-Raphson algorithm to solve the matrix of nodal equations when the circuit contains nonlinearity such as physical models of switches and diodes. The second class includes the discrete-transition simulators such as PSIM and others [2]-[5]. PSIM for example uses the nodal analysis with the trapezoidal rule integration algorithm. The simplicity of their components and the fact that they disregard the transition instances makes the discrete transition simulators much faster than the SPICE based simulator and eliminate, to a large extent, convergence problems. On the down side, since most discrete transition simulators do not apply full physical models of devices, they are incapable of showing parasitic processes. For example, diodes in PSIM are ideal and include only one parameter, forward diode voltage drop. Consequently, simulation results are unrealistic (Fig. 1) when simulating some power electronics circuits such as snubbers that are affected by non ideal and parasitic properties. Additionally, discrete-transition tools are running with fixed time steps. Thus, in order to distinguish short event processes, very small time step is required.

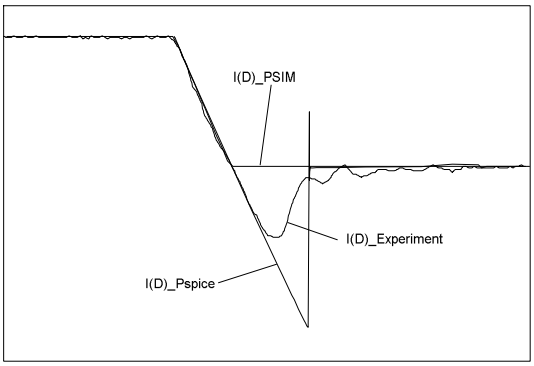

Fig. 1. Experimental and simulated turn-off current waveforms of a power diode (PSIM disregards reverse recovery process).

The objective of this study was two fold. First, to develop a modeling strategy for simulating the diode reverse recovery process within discrete-transition simulators. The second objective was to investigate a three-phase buck-type rectifier [6] that includes a lossless turn-on snubber with the aid of the proposed model.

II. MODELING PROCEDURE AND PARAMETERS EXTRACTION

Lauritzen and Ma *et. al.* [7] proposed a simple diode model that includes the reverse recovery process. The model is based on the lumped charge control concept and is relatively simple as compared to other numerical models [8] that include a large number of parameters and lead therefore to a long simulation time. The method adopted in this study is based on the lumped charge control concept. This principle is described analytically by the following equations:

$$i_{\mathrm{D}}(t) = \frac{q_{\mathrm{e}} - q_{\mathrm{m}}}{T_{\mathrm{m}}} \tag{1}$$

$$0 = \frac{dq_{\mathrm{m}}}{dt} + \frac{q_{\mathrm{m}}}{\tau} - \frac{q_{\mathrm{e}} - q_{\mathrm{m}}}{T_{\mathrm{m}}} \tag{2}$$

$$q_e = I_S \tau \left[\exp(\frac{v_D}{n V_T}) - 1 \right] \quad (3)$$

where, $i_D(t)$ is the diode current, q_e is the injected charge level at the junction, q_m is the total forward bias injected charge, T_m is the drift region transit time, τ is the life time, I_S is the diode saturation current, v_D is the diode junction voltage, V_T is the thermal voltage and n is the emission coefficient.

For efficient simulation time realization it is necessary to minimize computational overheads as much as possible. Hence, the model was further simplified in this study by disregarding the exponential dependency between the forward voltage v_D and the charge q_e of the power diode (3). In the derivation process of the model, only the reverse recovery was included while the forward voltage drop of the diode is considered fixed parameter. The proposed equivalent circuit model of Fig. 2 (implemented in PSIM, Version 8) emulates the physical behavior during the turn-off period of a typical power diode. The first order differential equation (2) is emulated in the model by an RC network. The resistor–capacitor pair RtauCtau of the model reflects a time constant τ during $0 < t < t_a$ (Fig. 3). The resistor–capacitor pair Rtau_rrCtau reflects a time constant τ_{rr} during the recovery period $t > t_a$. E_id is a current controlled voltage source associated with the diode current and equal to $\tau \cdot i_D(t)$. The voltage controlled current source G_qm expresses the response $q_m(t)/T_m$. The role of the switch SW_rr is to select the correct time constant and is controlled by the state of the ideal diode D_vf. The diode D_vf carries the sum of $i_D(t) + q_m(t)/T_m$. As long as D_vf conducts, the switch SW_rr is 'off' and the time constant is τ. According to reference [7], at time

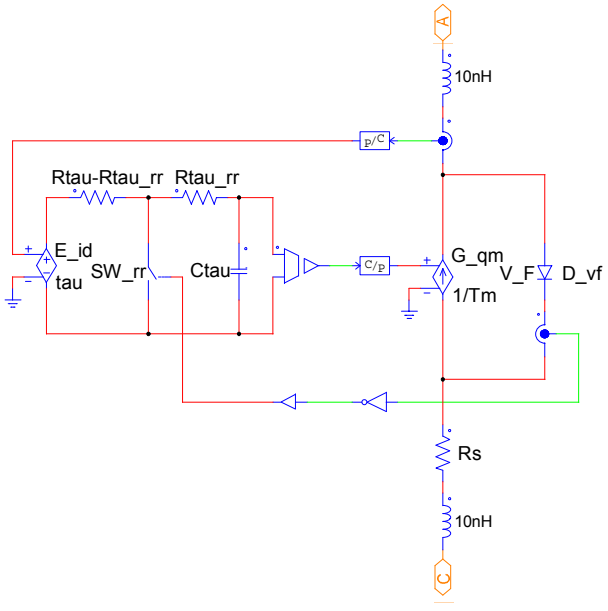

Fig. 2. Proposed diode model with reverse recovery (PSIM implementation). The 10nH inductor represents a parasitic lead inductance.

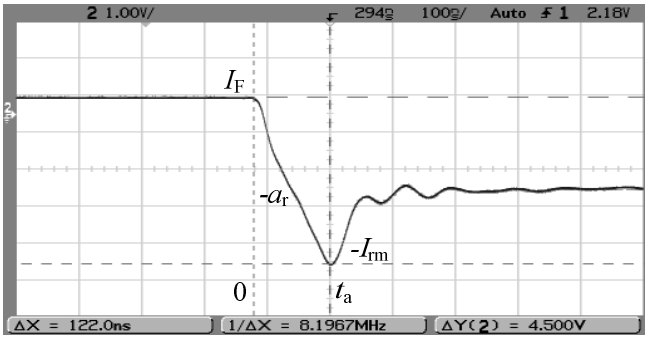

Fig. 3. Experimental turn-off current waveform of power diode (MUR8100E, ON-Semi) with stray inductance (L_s = 1.35µH, I_F = 2.5A, I_{rm} = 2A, a_r = $\Delta Y/\Delta X$, $t_a = \Delta X$). Vertical scale: 1A/div., horizontal scale: 100nsec/div..

instant t_a the diode current $i_D(t_a)$ and $q_m(t_a)/T_m$ have equal magnitude with opposite sign. At this instant, D_vf stops conducting and the switch SW_rr turns on. From now on the current $i_D(t)$ will decay to zero with a time constant τ_{rr} as follows,

$$i_D(t) = -I_{rm} \exp(-\frac{t - t_a}{\tau_{rr}}) \quad (4)$$

where I_{rm} is the peak reverse current (Fig. 3).

Seven model parameters need to be determined in the following order. The fundamental parameters τ_{rr}, τ and T_m must be extracted first by measurement. The parameter τ_{rr} can be obtained by fitting (4) against measurement data over $t > t_a$. In [7], it is shown that the following relationships holds,

$$I_{rm} = a_r (\tau - \tau_{rr}) \left[1 - \exp(-\frac{t_a}{\tau}) \right] \quad (5)$$

$$\frac{1}{\tau_{rr}} = \frac{1}{\tau} + \frac{1}{T_m} \quad (6)$$

where a_r is the current fall slope (Fig. 3).

By substituting the experiment parameters I_{rm}, a_r, t_a, τ_{rr} into (5) one can extract τ. T_m is calculated from τ and τ_{rr} using (6). Once the fundamental parameters are extracted, the calculation of the model parameters may proceed as follows: The contact resistance Rs = $\Delta v_D/\Delta i_D$ (from diode forward static characteristic), V_F = V_F (from diode forward static characteristic), Tm = T_m, tau = τ, Ctau = C_o (arbitrary number), Rtau = τ/C_o and Rtau_rr = τ_{rr}/C_o.

III. Model Verification

The diode tested in the experiments is a commercial fast recovery power diode MUR8100E, (ON-Semi.) with a nominal reverse recovery time of 75nsec. Test measurements were carried out with an estimated reverse voltage of 50V during the turn off period of the diode. Fig. 3 represents an example of a typical turn off waveform in the presence of stray circuit inductance with the following experimental parameters: initial forward current I_F = 2.5A, peak reverse

current I_{rm} = 2A, current fall slop a_r = 4.5A/122nsec and the length of the turn off period t_a = 122nsec. The estimated stray inductance L_s was found to be 1.35µH. Applying the proposed extraction method, the extracted model parameters were found to be: Rs = 50mΩ, V_F = 1V, Tm = 75.33nsec, tau = 144.8nsec, Ctau = 1nF, Rtau = 144.8Ω and Rtau_rr = 49.55Ω (τ_{rr} was estimated according to Fig. 4). The comparison between the experimental and simulated results of the proposed model for various turn off conditions including various forward currents and different stray inductances is shown in Fig. 5. The figure shows a good fit of the simulation to the experimental data. The model gives good results for forward currents below 2.5A and exhibit a reasonable accuracy for a forward current of I_F = 4.3A (Fig. 5 (f)). The deviation can be explained by the fact that the parameters were fitted to give closest approximation to the data in Fig. 3 in which the forward current was I_F = 2.5A. In addition, a slow decay of the tail to zero was observed. This is probably because the single time constant of the model is incapable of simulating accurately multi part decay waveforms [9].

The model was also tested in a dc-dc buck converter that includes a passive lossles snubber network as shown in Fig. 6. The objective of this verification stage was to anticipate snubber operation before applying it to a three-phase rectifier in which the main output inductor L_o is tapped. In the experimental circuit: V_{in} = 50V, V_o = 12V, P_o = 30W, f_s = 24KHz, L_r = 2µH, C_r = 10nF, D_{aux1} and D_{aux2} were MUR415 (ON-Semi). The converter was digitally controlled by dsPIC30F2020, which in the simulation is represented by a C

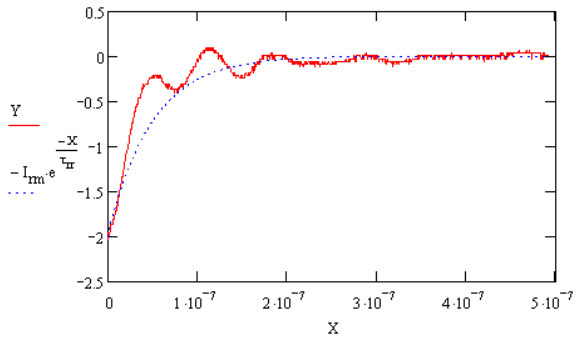

Fig. 4. Extracted reverse recovery time constant τ_{rr}.Y is the measurement data during $t > t_a$ and the dashed curve corresponds to the fitting of equation (4) with the following outcomes: I_{rm} = 2A and τ_{rr} = 49.55nsec.

block (Fig. 6). The simulation was conducted using the following assumptions: (1) auxiliary diodes D_{aux1} and D_{aux2} are ideal with constant forward voltage, (2) reverse recovery effects of only the main freewheeling diode is considered. Simulation results and the experimental verification waveforms are depicted in Fig. 7. The simulation model replicated very well the behavior of the experimental circuit, except for some negligible differences. The small discrepancy between the measured and simulated waveforms could be the result of stray capacitance and inductance as well as due to the fact that the forward voltage of the diodes in the simulation circuit and the experimental one were not exactly the same. As expected, large deviations are found between experiment and simulation when the original PSIM diode is used (Fig. 7 (b)).

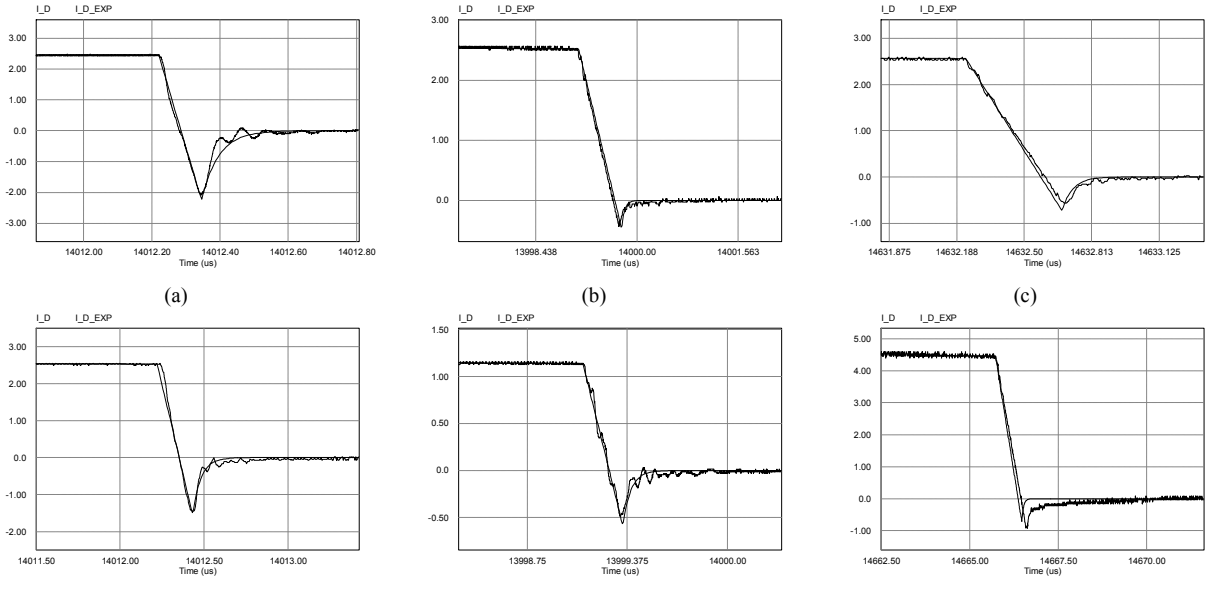

Fig. 5. Reverse recovery model validation (PSIM simulation). (a) Comparison to the measurement curve of Fig. 3, (b) L_r = 10µH, I_F = 2.5A, (c) L_r = 6µH, I_F = 2.5A, (d) L_r = 1.3µH, I_F = 2.5A, (e) L_r = 6µH, I_F = 1.3A, (f) L_r = 6µH, I_F = 4.3A.

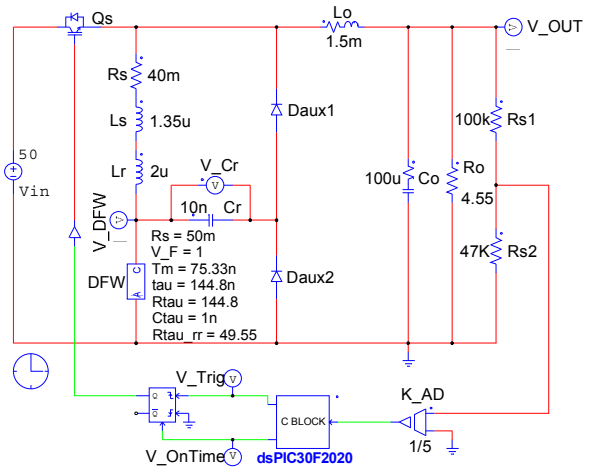

Fig. 6. Circuit diagram of simulation and experimental setup of dc-dc buck converter. L_r and L_s are the snubber inductor and stray inductance, respectively.

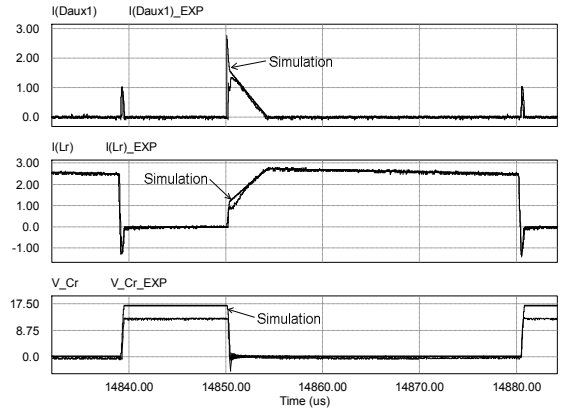

(a)

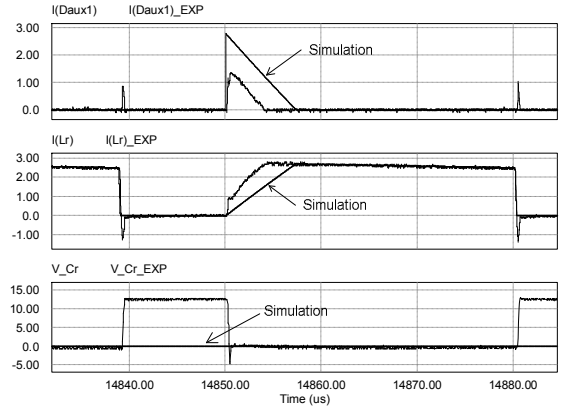

(b)

Fig. 7. Comparison between simulation (PSIM) and the experimental waveforms of the turn-on lossless snubber: (a) results when the proposed diode model is included, (b) the results when the original PSIM diode is used.

IV. Exploring Lossless Snubber for Three-Phase Buck-Type Rectifier

The reverse recovery process is often a significant source of loss in hard switched converter as well as a major EMI generator. The hard switching of the freewheeling diode in buck converter induces power loss in the main transistor [10], given approximately by,

$$P_{sw} \cong V_{in} f_s \left(Q_{rr} + t_{rr} I_o \right) \tag{7}$$

were, V_{in} is the input voltage, f_s is the switching frequency, Q_{rr} is the recovered charge during t_{rr} period, and I_o is the output current. This loss mechanism exists also in three-phase buck-type rectifier except that V_{in} cannot be considered constant as in (7). A comprehensive analysis of turn-on lossless snubber for DC-DC Boost converter was presented in [11]. The objective of the present study was to demonstrate a practical application of the proposed diode recovery model by investigating this type of lossless snubber when implement in a three-phase buck-type rectifier (Fig. 8). At high switching frequencies, the free wheeling diode D_{FW} in Fig. 8 produces significant reverse recovery related losses (7) when the main switches Q_R, Q_S, Q_T are under "hard" switching condition. The key to the design of the circuit shown in Fig. 8 is to minimize the circuits reverse recovery losses in order to maximize system efficiency. It is shown in [11] that these losses can be minimized when the turn-off di/dt rate of the main diode D_{FW} is controlled by a series inductor L_r. At the same time, the conduction period of the snubber diodes D_{aux1}, D_{aux2} must be minimized otherwise they may conduct the full output current I_o. In order to reduce the conduction period of the snubber diodes, the designer need to take into consideration the trade off between snubber components values and the magnitude of I_{rm}. It has been shown in [11], that for proper operation $I_{rm} > I_o$, in which case the conduction of the snubber diodes will be minimal. This optimization can be conveniently done by simulation.

The output voltage of the three-phase rectifier is described by the following equation [6],

$$V_o = \frac{3}{2} M U_m \cos\varphi \tag{8}$$

where M is the modulation index, U_m is input voltage amplitude and φ is the displacement angel between mains phase current and voltage. The simulation was carried out by considering only the reverse recovery effect of the main freewheeling diode. In addition, the analysis was conducted with coupled inductors circuit in which the snubber inductor L_r is coupled to the main inductor L_o (Fig. 8). This configuration helps to extend the operation of the snubber over a wider duty cycle range [11]. In order to reduce computation overhead during simulation, the coupling has

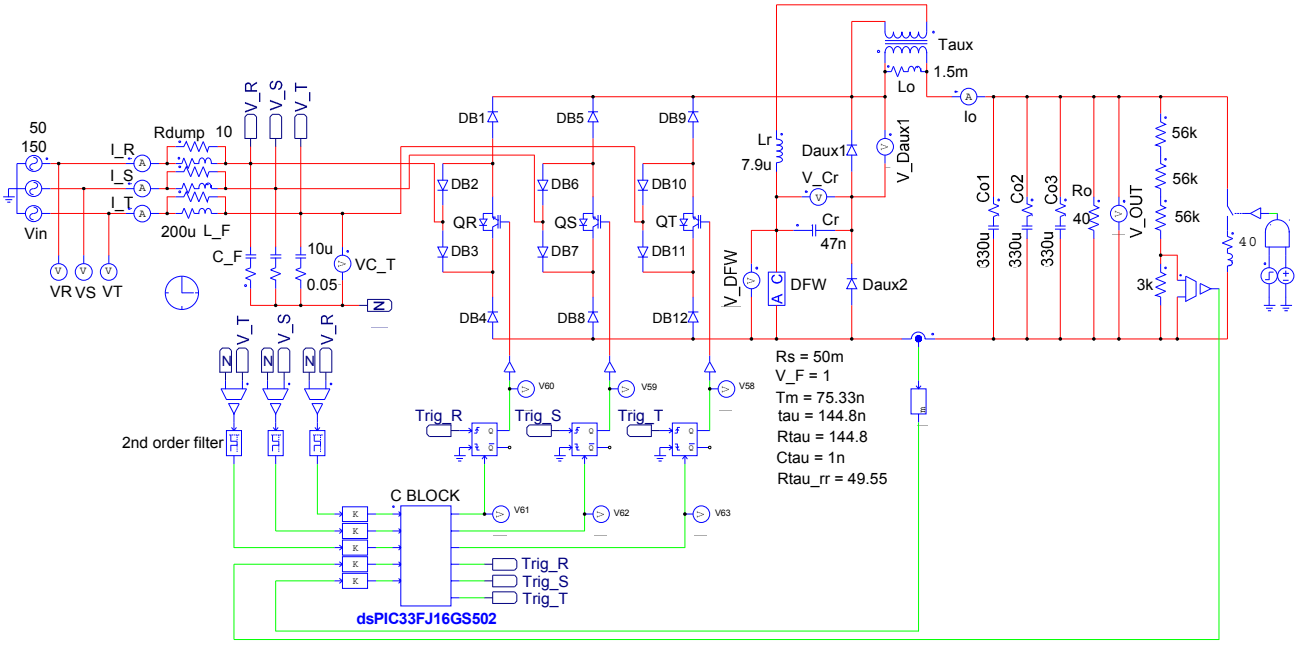

Fig. 8. Simulation and equivalent experimental circuit diagram of lossless turn-on snubber applied to a three-phase buck-type rectifier. The snubber inductor L_r is coupled to the main inductor L_o.

been implemented by an ideal transformer T_{aux} (Fig. 8). The parameters of the proposed diode model correspond to the experimental data of Fig. 3. The AC side and DC side simulated waveforms of the rectifier are shown in Fig. 9. The simulated waveforms of the snubber when embedded in the three phase rectifier are depicted in Fig. 10. This figure can be helpful in defining the required ratings of circuit components. For instance, as evident from Fig. 10 (b), about 160V is developed across D_{aux1} during the reverse recovery period. Therefore, this diode must be able to withstand reverse voltage of at least 200V. The experimental components and parameters are summarized in TABLE I. A three-phase variable voltage source was applied to the

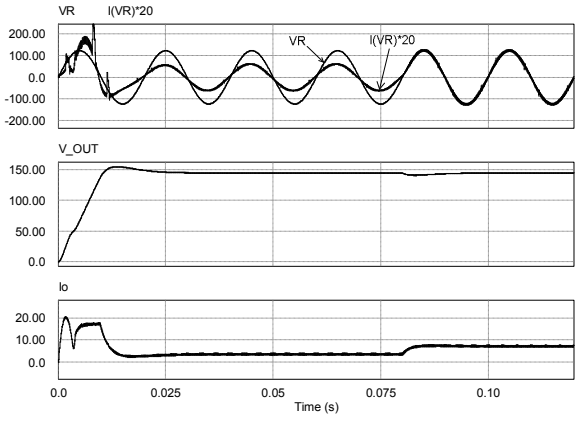

Fig. 9. AC side (top trace) and DC side (middle and bottom traces) simulated waveforms (PSIM) of the three-phase rectifier.

rectifier that was loaded by a resistive load. The coupled inductor was implemented with double E65 core. The measured value of the leakage inductance at the secondary terminals was 7.9μH. The control of the rectifier was realized by a 16-bilt 40 MIPS digital signal controller dsPIC33FJ16GS502. Fig. 11 and Fig. 12 show various experimental waveforms recorded for the given setup conditions. Phase current and voltage are shown in Fig. 11. Fig. 12 (a) and Fig. 12 (b) show voltage and current of the freewheeling diode D_{FW} and snubber diode D_{aux1} respectively.

V. Discussion and Conclusion

The proposed diode reverse recovery model is suitable for very detailed study of device interactions with the rest of the circuit, e. g., snubber design. The experiment results were found to be in good agreement with the simulation waveforms (Fig. 5). This good agreement justifies the approximation that was done in the development of the model (e. g. neglecting exponential dependency of the forward voltage v_D and the parameter extraction procedure that is based on a single measurement). The practical usefulness of the model over the standard ideal diode was demonstrated in a test bench dc-dc buck converter. The diode model was found to reproduce faithfully the experimental data (Fig. 7 (a)). It is well known that parameters extraction from several measurements will improve the precision of models. Nonetheless, as evident from Fig. 5, the parameters extraction from a single measurement, as explored it this study, gives a very good starting point for predicting behavior in different

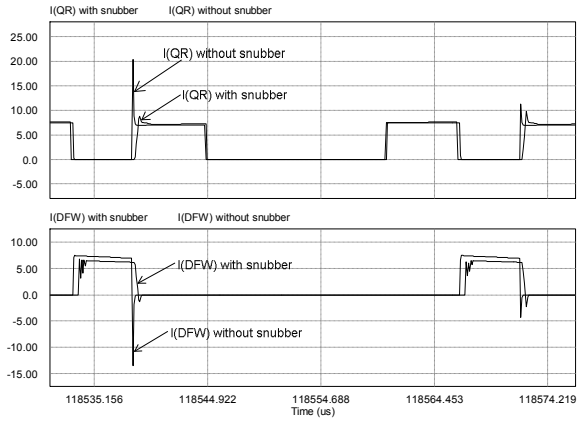

(a)

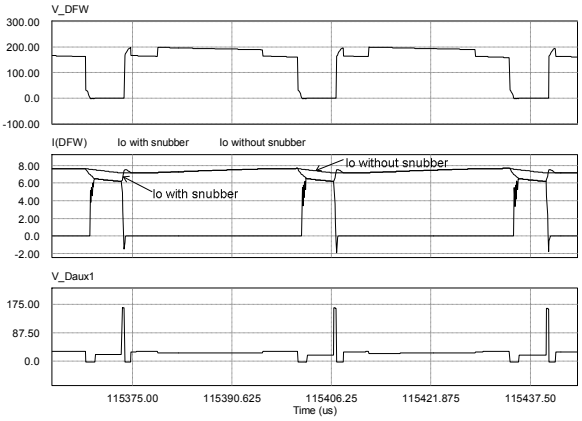

(b)

Fig. 10. Key simulation (PSIM) waveforms of the lossless snubber under investigation. (a) Current waveforms of the switch (upper trace) and freewheeling diode (lower trace) with and without the snubber, (b) Traces from top to bottom: v_{DFW}, i_{DFW}, i_o, v_{Daux1}. (See Fig. 8).

operating conditions.

The performance of a lossless snubber applied to a three phase rectifier under different operating conditions was investigated. The simulation results with the proposed model predict a lower reverse recovery stress of the switches (Fig. 10 (a) and Fig. 12 (a)) which imply better efficiency [12], [13]. It is evident from Fig. 10 (b) that the output current ripple has increased because the total magnetizing current (referred to the primary winding) is equal to $i_{Lo} + i_{Lr} \cdot n_S/n_P$. This ripple increase needs to be taken into account in the design stage of the DC side inductor and the AC side input filter.

The simulation time in PSIM was recorded for the dc-dc converter and for the three-phase rectifier with the proposed diode model. In the dc-dc converter the computation time for open loop and closed loop simulations were, 9sec and 21sec respectively for 6msec total run time and 10nsec time step. In comparison, the cycle by cycle simulation running time of this circuit in Pspice in open loop configuration was 30sec for

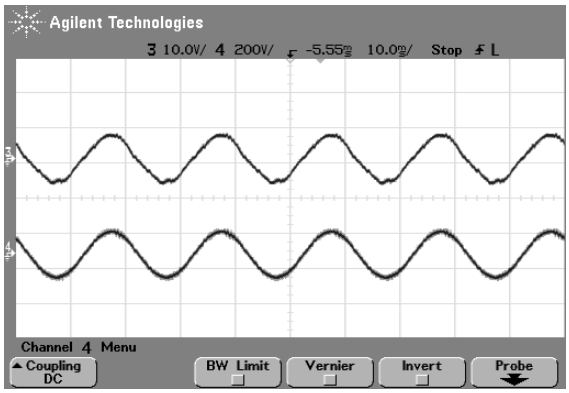

Fig. 11. Experimental waveforms: input phase current i_R (upper trace) and input phase voltage v_R (lower trace). Vertical scale (upper trace): 10A/div., Vertical scale (lower trace): 200V/div., horizontal scale: 10msec/div.. (See Fig. 8).

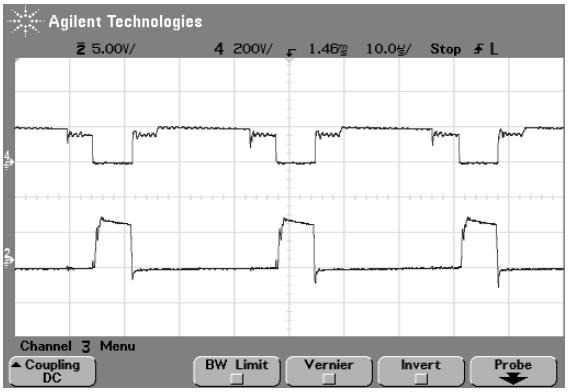

(a)

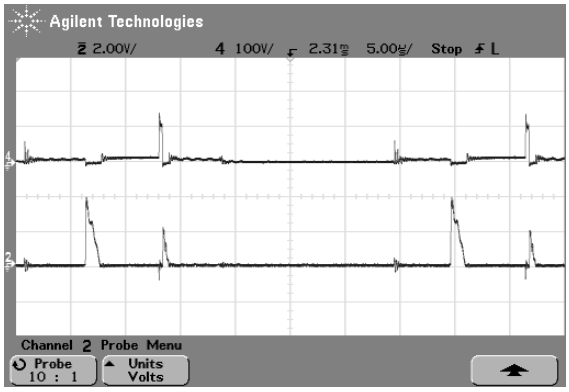

(b)

Fig. 12. Experimental waveforms: (a) freewheeling diode waveforms, v_{DFW} (upper trace) and i_{DFW} (lower trace). Vertical scale (upper trace): 200V/div., Vertical scale (lower trace): 5A/div., horizontal scale: 10µsec/div. (b) auxiliary snubber diode waveforms, v_{Daux1} (upper trace) and i_{Daux1} (lower trace). Vertical scale (upper trace): 100V/div., Vertical scale (lower trace): 2A/div., horizontal scale: 5µsec/div. (See Fig. 8)

the same 6msec total run time in which, the snubber diodes were represented by Dbreak diode and the main diode was a library diode model of MUR8100. For the three-phase rectifier, the PSIM simulation time for closed loop

TABLE I
CIRCUIT COMPONENTS AND PARAMETERS OF THE THREE-PHASE RECTIFIER EXPERIMENTAL SETUP

Mains line voltage	V_{LL}	150Vrms
Mains frequency	f_m	50Hz
AC side capacitor	C_F	10μF
AC side inductor	L_F	200μH
AC side dumping	R_{dump}	10Ω
DC side capacitor	C_o	990μF
DC side inductor	L_o	1.5mH
Modulation index	M	0.8
Switching frequency	f_s	30KHz
Output voltage	V_o	145V
Output power	P_o	1KW
Bridge switches	Q_R,Q_S,Q_T	IRG4PH50K
Bridge diodes	D_B	MUR8100
Freewheeling diode	D_{FW}	MUR8100
Snubber diodes	D_{aux1},D_{aux2}	MUR440
Snubber capacitor	C_r	47nF
Leakage inductor	L_r	7.9μH
Turns ratio	n_P:n_S	70:11

configuration was 3min and 39sec with the proposed diode model for 20nsec time step and 50msec total run time. In comparison, for the same conditions but with the use of the original diode of PSIM a computation time of 3min and 16sec was recorded. Hence, the use of the proposed model does not increase significantly the simulation time. Additional run time improvement could be achieved by activating the snubber (including the proposed model) after the circuit has reached steady state condition.

The strength of the model is in the ability to help designers to examine physical phenomena as reverse recovery and its interaction with other circuit components and at the same time to explore control needs for stability, soft switching and others on one platform.

Although demonstrated by PSIM implementation, the model can easily be incorporated in other discrete-transition power electronics simulators by following the proposed model construction procedure. The simulation methodology could be helpful in studying other reverse recovery problems such as losses due to internal drain-source body diode of a typical power MOSFET.

ACKNOWLEDGMENT

This research was supported by THE ISRAEL SCIENCE FOUNDATION (grant No. 476/08) and by the Paul Ivanier Center for Robotics and Production management.

REFERENCES

[1] Cadence Design Systems, Inc..
[2] *PSIM user manual*, Powersim Inc., Version 8.0, 2009.
[3] CASPOC [Online]. Available: http://www.integratedsoft.com/Caspoc
[4] PowereSIM [Online]. Available: http://www.powerEsim.com
[5] SIMPLIS [Online]. Available: http://www.simplistechnologies.com
[6] M. Baumann, U. Drofenik, and J.W. Kolar, "New wide input voltage range three-phase unity power factor rectifier formed by integration of a three- switch buck-derived front-end and a DC/DC boost converter output stage," in *Proc. IEEE-INTELEC Conf.*, 2000, pp. 461–470.
[7] P. O. Lauritzen, and C. L. Ma, "A simple diode model with reverse recovery," *IEEE Trans. Power Electron.*, vol. 6, no. 2, pp. 188–191, Apr. 1991.
[8] C. M. Tan, and K. J. Tseng, "Using power diode models for circuit simulation – A comprehensive review," *IEEE Trans. Ind. Electron.*, vol. 46, pp. 637–645, June 1999.
[9] M. D. Reid, S. Round, and R. Duke, "Modeling the temperature dependent reverse recovery behavior of power diodes," in *Proc. International Power Electronics Conf.*, 2000, pp. 779-783.
[10] R. W. Erickson, D. Maksimovic, *Fundamentals of power electronics*, 2nd ed., Springer, 2001, pp. 763-765.
[11] H. Levy, I. Zafrany, G. Ivensky, and S. Ben-Yaakov, "Analysis and Evaluation of a Lossless Turn-On Snubber," in *Proc. IEEE Applied Power Electronics Conf.*, 1997, pp. 757-763.
[12] G. R. Kamath, "A passive coupled inductor flying capacitor lossless snubber circuit for plasma cutting power supply," in *Proc. IEEE Applied Power Electronics Conf.*, 2005, pp. 237-243.
[13] M. Ilic, and D. Maksimovic, "Interleaved zero-current-transition buck converter," *IEEE Trans. Ind. Applicat.*, vol. 43, pp. 1619-1627, Nov./Dec. 2007.